αIIb-β3 integrin mutations in 24 Glanzmann Thrombasthenic patients and 2 carriers : Characterization of 18 new allelic variants and their effects on splicing and structure-function of the complex.

V. JALLU[1], M. DUSSEAUX[1], S. PANZER[2], M.F. TORCHET[3], N. HEZARD[4], J. GOUDEMAND[5], A.G. De BREVERN[6], C. KAPLAN[1]

[1] Platelet Immunology Laboratory, INTS, Paris, France

[2] Clinical Department for Blood Group Serology, Medical University of Vienna, Austria

[3] Centre des Hémophiles, Groupe Hospitalier Necker-Enfant malade, Paris, France

[4] Laboratoire d'Hématologie, CHU Robert Debré, Reims, France

[5] Hopital Cardiologique, Centre Hospitalier Régional Universtaire, Lille, France

[6] Dynamique des Structures et Interactions des Macromolécules Biologiques, INSERM UMR-S 665, University Paris Diderot - Paris 7 , Paris, France

Short title :

New mutations in Glanzmann patients and carriers

Correspondance

Dr Cécile KAPLAN

Laboratoire d'Immunologie Plaquettaire

INTS

6, rue Alexandre Cabanel

75015 Paris, France

Email : ckaplan@ints.fr

Phone : 33 1 44 49 30 66 Fax : 33 1 45 67 19 30

Abstract

Glanzmann thrombasthenia (GT) is an autosomal recessive inherited bleeding disorder characterized by an impaired platelet aggregation. GT results either from quantitative or functional defects in integrin αIIb-β3, the platelet fibrinogen receptor. Characterization of GT mutations is of interest for prenatal diagnosis and genetic counselling. Furthermore, they provide useful tools for structure-function relationship studies of the αIIb-β3 complex. Mutations from 24 GT patients and 2 carriers of various origins, Caucasian, North-African and Asian, referred for GT to our laboratory were characterized. Promotors and exons sequences of αIIb and β3 genes from DNA samples were amplified and directly sequenced. From these 26 propositi, 18 (60%) of the 30 mutations identified have never been characterized. For new αIIb allelic variants, 2 affect RNA splicing sites, 2 provoke frameshift and premature stop codon, 4 result in stop codon and 4 lead to amino acid substitutions. For β3, 2 were predicted to affect RNA splicing and 4 lead to amino acid substitutions. Two allelic variants of αIIb were identified in several unrelated propositi. RNA maturation alterations were evaluated by Genscan, NNSPLICE and ESEFinder online tools. The role of the 7 newly described missense mutations was analysed by expressing mutant complexes in transiently transfected Cos-7 cells. The substitutions Ser926Leu, Val903Phe of αIIb, and Cys38Tyr, Met118Arg, Gly221Asp and Lys253Met of β3 prevented normal expression of the complex. None of the single point base substitution leading to these allelic variants was predicted to alter mRNA splicing. The Gln595His substitution allowed complex expression but its corresponding c.2800G>T mutation prevents normal RNA splicing in *in silico* prediction. Using free energy analyses applied on the resolved structure of αIIbβ3, the Lys253Met substitution of β3 helped to define a key role of the Lys253 in the interaction of the αIIb β-propeller and the β3 β-I domains.

Keywords

αIIbβ3, ITGA2B, ITGB3, integrin, Glanzmann, splicing, modelization, structure-fonction

INTRODUCTION

Glanzmann thrombasthenia (GT) is an autosomal recessive bleeding disorder characterized by a prolonged bleeding time and an impaired platelet aggregation in response to physiological agonists such as ADP, thrombin, collagen and epinephrine {Caen, 1972 819 /id}. GT results from quantitative and / or qualitative defects of the fibrinogen platelet receptor, the glycoprotein αIIbβ3 complex. Classically GT has been divided in 3 subtypes defined by the αIIbβ3 content of patient's platelets : Type I, no or only trace amounts of αIIbβ3; Type II and variant, respectively with low and near normal platelet surface content of functionally impaired αIIbβ3 {Nurden, 2005 1776 /id}. To date more than 60 mutations involved in GT phenotype have been described in the αIIb gene and more than 40 in the β3 gene. The nature of GT mutations is highly variable excepting some that are commonly indentified in consanguineous populations such as the αIIb c.409-3_418del (IVS3-3del13) and the β3 c.2031_2041del (2031del11) respectively detected in Arab and Iraqi-Jewish GT populations {Newman, 1991 836 /id}, the αIIb c.1544+1G>A (IVS15+1/G>A) mutation in French Gypsies {Schlegel, 1995 911 /id}, or the β3 c.1053_1058del (1053CCCAGG) deletion in North-Africans {Morel-Kopp, 1997 1064 /id}.

Characterization of GT mutations in patients is critical for prenatal diagnosis and genetic counseling. We report here the characterization of 30 mutations identified in 24 thrombasthenic patients and 2 asymptomatic carriers. Using site directed mutagenesis, cell expression models, *in silico* tools and the resolved stucture of the αIIbβ3 complex, we have depicted the pathogenic role of 18 newly described allelic variants. This study has revealed

the importance of the Lys253 in the interaction of the αIIb β-propeller and the β3 β-I domains.

MATERIAL AND METHOD

Patients

Blood samples from patients were sent to our laboratory for confirmation of GT diagnosis and genetic analysis. Propositus 4 and 15 are GT carriers. Patient 4 who presented with a mild bleeding disorder discovered during surgery was adressed to the laboratory for GT investigation after flow cytometric analysis revealed a 50 % reduction of αIIb-β3 platelet surface expression. The propositi and their platelet phenotype are listed in table 1. None of these patients have been previously studied for molecular gene defects.

Monoclonal antibodies

Monoclonal antibodies (Moab) SZ1 (anti-GPIX), SZ22 (Anti-αIIb), SZ21 (Anti-β3), P2 (Anti-αIIb-β3) and E3 (anti-fibrinogen) were purchased from Beckmann Coulter-France (Villepinte, France). Moabs AP2 (Anti-αIIb-β3) and AP3 (Anti-β3) were obtained from Lucron Bioproducts (Lille, France). The Moab XIIF9 to β3 was a generous gift from G.Vezon (CRTS, Bordeaux, France). In some flow cytometry experiments the Moabs SZ22, SZ21 and P2 were directly conjugated to FITC.

Blood samples

Blood samples from patients were collected by venipuncture using 5mM ethylene-diamine-tetra-acetic acid as an anticoagulant. Platelet were separated by differential centrifugation and

used or stored in 70% ethanol at –80°C until RNA was extracted. In some cases, 500 µl of whole blood were mixed with 1.3 ml of RNA Later (Applied Biosystem, Courtaboeuf, France) and were kept frozen at –80°C for subsequent RNA extraction.

Flow cytometry

For platelets' glycoproteins and fibrinogen content analysis, 50 µl of EDTA anticoagulated whole blood was diluted in 500 µl of phosphate saline buffer (PBS) pH 7.2 containing 1 % (wt/vol) BSA-fraction V (Euromedex, Souffelweyersheim, France) and 3 mM EDTA (PBE buffer). Cell were fixed by adding 1.5 ml of PBS-3mM EDTA, pH 7.2, containing 1.33 % (vol/vol) of a methanol-stabilized formaldehyde solution (Fisher Scientific, Illkirch, France) for 15 mn at room temperature (RT). The reaction was stopped by adding 2 ml of PBE before cells were pelleted by centrifugation at 1500 g for 10 mn. Pelleted cells were washed in 2 ml PBE before to be resupended in 1 ml PBE containing 0.1 % (wt/vol) sodium azide and store at 4°C until use. 40 µl of the fixed cells suspension were incubated with 3 µg/ml Moab in PBE (qsp 100 µl) for 1 h at RT. After two washes in 2 ml PBE, the bound Moabs were detected by using a polyclonal goat anti-mouse IgG conjugated to FITC (Jackson Immunoresearch Europe, Newmarket, UK) 1/10,000 diluted in PBE for 30 mn at RT. Following one wash in 2 ml PBE, mean fluorescence intensity of cells was analyzed on an XL-MCL Flow cytometer (Beckman Coulter, Villepinte, France). To detect intraplatelet fibrinogen, each incubation steps were done in presence of 1% (wt/vol) saponine (Fischer Scientific). Amounts of proteins are expressed as a percentage of the mean amounts obtained with normal platelets from several healthy donors.

To analyse αIIβ3 wild type or mutant complexes express at the suface of transfected Cos-7 cells, cells were collected by Trypsin-EDTA treatment and washed 2 times in PBS-1%

(wt/vol) BSA. 5 x 10^5 cells were incubated in 100 µl PBS containing 3 µg/ml Moabs SZ22, SZ21 or P2 conjugated to FITC for 1 h at RT. Cells were washed 2 times in 2 ml PBS-BSA before to be analyzed on the Flow cytometer. Dead cells were discarded from analysis by using the 7-AAD viability dye (Beckmann-Coulter). Results are expressed as a percentage of positive cells for the concerned antigen.

DNA/RNA extractions

Genomic DNA was isolated from peripheral blood according to a published procedure {Jallu, 2002 1521 /id} or by using the MagNA Pure Compact Instrument and the Nucleic Acid Isolation Kit I (Roche Diagnostics, Meylan, France). In some cases, DNA samples were obtained by using QIAamp DNA Blood Mini kit (Qiagen, Courtaboeuf, France). RNA extractions were done on platelets by using the Rneasy Protect MiniKit (Qiagen). DNAs and RNAs were extracted according to the manufacturers' instructions.

Sequencing analysis

Sequencing was performed as previously described {Quintanar, 1998 1330 /id} or by GenoScreen (Lille, France). Primers defined by Kato and coworkers {Kato, 1992 828 /id} and Jin and co-workers {Jin, 1993 1164 /id} were respectively used to amplify coding sequences of αIIb and β3 genes from genomic DNA. Primers to amplify promotor sequences of αIIb and β3 have been respectively defined according to the genes' reference sequences NG_008331.1 and NG_008332. αIIb promotor sequences were studied by using the following primer pairs ("a" forward, "b" reverse):

IIbP1a CGCCAGAATTCTCAGTCACGAAGCTTGGCTCAAGACGGAG

IIbP1b CCAGCCAGATATCAGCTATGTACTACCACCGTGCTAGTCC

IIbP2a CGCCAGAATTCTCAGTCACGGGTAAAGATTCAAGAGACAT

IIbP2b CCAGCCAGATATCAGCTATGTCAGATTCCTCCACAGGAAG

IIbP3a CGCCAGAATTCTCAGTCACGGAAGGGAAGGAGGAGGAGCT

IIbP3b CCAGCCAGATATCAGCTATGCTTCCCTTACGGCTCACCTC

Underlined sequences are non genomic sequence for sequencing PCR products. Promotor and exon 1 sequences of β3 gene were amplified with the primer pair

IIIaE1a ATGTGGTCTTGCCCTCAACAGGTAG

IIIaE1b CACGCTCTCACCCAGGAAGTTACAG by using the Advantage GC genomic PCR kit (Clontech, Saint-Germain-en-Laye, France) and then sequencing was done with the forward primer 3aseq-P1a CCGGAAAACCAAACTAAGGC and the reverse primer 3aseq-P1b GACCAGTCCTCCGCGTTTGC.

All identified mutations were confirmed by PCR-Restriction Fragment Length Polymorphism (PCR-RFLP) analysis on a second amplicon. Restriction enzymes are listed in tables 2 and 3 with the corresponding mutations. The experimental details of these RFLP assays can be obtained upon request. When the mutation did not introduce restriction modification, sequencing was done on a second PCR-product. For nucleotide numbering the A nucleotide of the ATG start was designated +1 (cDNA ITGA2B and ITGB3 GenBank accession numbers NM_000419.3 and NM_000212.2 respectively). For amino acid numbering used in the text, the first amino acids of the mature αIIb and β3 proteins were designated +1. Residue numbering according to the HGVS nomenclature that designed as +1 the translation initiating Methionine (http://www.hgvs.org/mutnomen) is also shown in tables 2 and 3. Both numberings differ by 31 and 26 residues that correspond to the signaling peptides of αIIb and β3 respectively.

Site directed mutagenesis and in-vitro expression

Site directed mutagenesis, *in vitro* expression in Cos-7 cells were done as previously described {Jallu, 2002 1521 /id} or by using the QuikChange® II XL Site-Directed Mutagenesis Kit (Agilent Technologies, Massy, France) according to the manufacturer's instructions. In some mutagenesis experiments, the plasmid pcDNA3.1-Zeo containing the αIIb cDNA was used instead of pcDNA3.1-Neo (Invitrogen, Cergy Pontoise, France).

Western-blot analysis

Trypsine-EDTA collected Cos-7 cells were washed 2 times in PBS and 1 time in 50 mM Tris-HCL pH 7.6, 150 mM NaCl. Cells were resuspended (1.5 x 10^7 cells) in 100 µl of the same Tris buffer containing 1% (wt/vol) Triton-X 100 and 2 mM para-Methyl Sulfonyl Fluoride (PMSF). They were lysed for 30 mn at 4°C and the lysate rotated at 16.000 g for 30 mn at 4°C. The supernatant was diluted with 4 volumes of a 150 mM NaCl solution containing 2.5 % (wt/vol) Sulfate Dodecyl Sodium (SDS), 31.25 mM n-ethylmaleimide and 2.5 mM PMSF. The SDS lysate was heated to 100°C for 5 mn before 35 µl were used for western-blot analysis as previously described {888} with a minor modification : bound antibodies were detected by using anti-mouse IgG conjugated to the peroxidase associated to the chemiluminescence detection technique.

Computational analyses

The effect of mutations on intron splicing has been predicted *in silico* by using the following tools : Genscan (http://genes.mit.edu/GENSCAN.html {Burge, 1998 2007 /id}) and NNSPLICE 0.9 (http://www.fruitfly.org/seq_tools/splice.html {Reese, 1997 1914 /id}).

Modifications of the splicing factors binding sites pattern resulting from the mutations were evaluated by using the ESEFinder tool {Cartegni, 2003 2005 /id;Smith, 2006 2006 /id}.

To compare wild type and a mutant headpiece of αIIbβ3, modelization has been done using the structure (PBD code 2VDL) published by Springer et co-workers {2022}. A structural model of mutant has been built. It was checked using ProCheck software to analyze the quality of the modification {2026} and the side-chain position has been analysed with SCWRL {2025}. Finally, the FastContact web server (http://structure.pitt.edu/servers/fastcontact/) was used to estimate the direct electrostatic and desolvation interaction free energy between two proteins in units of kcal/mol {2023;2024}.

RESULTS

Clinical GT diagnosis was confirmed in our laboratory by immunologic or biochemical studies (See table 1). Genomic DNA samples from patients were studied for molecular defects in promotor and exons sequences of genes coding for αIIb and β3 by direct sequencing of the correponding PCR products. Identified allelic variations in these genes are reported in tables 2 and 3. To avoid erroneous identification due to amplification errors, all sequence alterations have been confirmed on a second PCR product either by a PCR-RFLP technique when a restriction site modification was observed or by new sequencing analysis in the other case. Restriction enzymes that have been used are listed in tables 2 and 3 with their corresponding allelic variant. When avalaible, DNAs from patient's relatives were also analysed and used to confirm the allelic variations (data not shown).

αIIb gene and mutations

For 18 propositi, a total of 23 mutations were identified in the gene coding for αIIb (See table 2). Two of these mutations were found in different probands.

♦ Five lead to nonsense codons, c.531T>A (Cys146stop), c.1413C>G (Tyr440stop), c.1563T > A (Cys490stop), c.1672C>T (Gln527stop) and c.2929C>T (Arg946stop), (patients 1, 6, 7, 8 and 17 respectively).

♦ Two point mutations directly affect a splice site : c.1879-2A>G (patient 9) and c.3060+2T>C (patient 12), as does the 13 base pair deletion, c.1442-13_1442-1del that has been identified for 3 unrelated propositi, GT patients 3 and 5, and the carrier 4.

♦ Two heterozygous single base insertions were identified in patient 2. These mutations, c.917_918insA and c.1912_1913insT, are predicted to result in frame-shift anomalies creating downstream stop codon 22 amino-acids (aa) later that leads to premature termination.

♦ Patient 14 presents an homozygous c.2748_2757del mutation that leads to a frame shift anomaly starting with the Thr886Ser amino acid substitution.

♦ Other identified gene anomalies affecting αIIb, were missense mutations. Three of them (patients 6, 10, 15 and 16) have not been described so far and 6 (Patients 3, 11, 12, 13 and 18) have already been reported (see references in the table 2).

Among the 9 heterozygous compounds, 4 second obligatory mutations (patients 5, 7, 17 and 18) remain to be identified (NI abbreviation (not identified) in tables).

Mutations detected in the β3 gene

Eleven mutations were identified in the gene coding for the β3 glycoprotein for 8 propositi (See table 3).

♦ The c.100C >T mutation (patient 20) is responsible for a nonsense codon R8X.

♦ The point mutation c.166-2A>G (patient 19) disrupts the acceptor splice site of the intron 2.

♦ An homozygous 4 base pair deletion located downstream of the donor splice site (c.1125+3_1125+6del) of intron 8 has been identified as the unique mutation in patient 25.

- In patient 26, two silent homozygous mutations, c.1143C>A and c.1260G>A (20507 C>A and 20624 G>A with genomic numbering) located in exon 9, were reported to be responsible for a type I GT {Jin, 1996 1293 /id}. Though silent, their association induces exon 9 skipping and the introduction of five intronic bases in the final transcript {Jin, 1996 1293 /id}. Analysis of the mRNA from the patient 26 has confirmed this deletion / insertion mechanism (data not shown).
- Six missense mutations were identified (Patients 21, 21, 23 and 24).

In 2 hétérozygous patients the second obligatory GT mutation remains be determined.

Flow cytometric analysis of mutant complexes expressed in Cos-7 cells

Seven missense mutations not previously reported in the literature have been further studied by expressing the mutant complexes in COS-7 cells to assess their role in the GT phenotype. Cell surface expression of the mutant complexes was assessed by flow cytometry usings Moabs to αIIb (SZ22), β3 (SZ 21) or to the αIIbβ3 complex (P2) (See fig 1).

- Mutations S926L (Patient 16) and V903F (Patients 6 and 15) affecting αIIb or mutations C38Y (patient 21), M118R (Patient 22), G221D and K253M (Patient 24) affecting β3, prevented normal complex expression, mimicking the type I GT phenotype observed for the patients. For the mutants αIIb S926L (Patient 16) and β3 G221D and K253M (Patient 24) the percentage of positive cells expressing β3 is slighty higher than in other mutants tested (See fig 1), except for the Gln595His. This low level expression could be correlated to the 10 % of β3 expression at the surface of the patients' platelets (See table 1).
- Unexpectedly the αIIb mutation Q595H (patient 10) did not reproduce in Cos-7 cells a type I GT phenotype as the expression of the mutant complex is similar to that obtained with its wild type form.

As controls, non-transfected cells did not bind significantly any of the Moabs tested and irrelevant mouse IgG gave less than 1% of positive cells whatever the transfectant tested.

Western-blot analysis of the effect of the C38Y β3 mutation on the complex expression.

Figure 1 revealed that the C38Y substitution strongly affect the complex expression but also that of β3 when tested with the anti-β3 Moab SZ21. To understand this specific effect, synthesis of the Y38β3 form of the complex in the transfected cells was analysed by using a Western-blot technique with Moabs SZ22 to αIIb and SZ21, XIIF9 and AP3 to β3 (See fig 2). SZ22 showed that αIIb is clearly detectable in the lysate of the wild type αIIb-β3 transfectant (lane c) like in the control platelet lysate (lane a). For the αIIb-Y38β3 mutant transfectant, only a band of slightly greater relative mobility that might correspond to a degradation product of αIIb was detected (lane d). The Moab XIIF9 revealed the presence of the Y38β3 mutant in the αIIb-Y38β3 transfectant (lane c). However, this mutant glycoprotein presents a lower relative mobility when compared to the wild type forms detected in lysates from platelets or wild type αIIb-β3 transfectant (lane c). Both SZ21 and AP3 failed to react with the Y38β3 mutant (lanes d) but reacted with normal β3 expressed in platelet and wild type αIIb-β3 transfectant (lanes a and c respectively). XIIF9 and AP3 but not SZ21 reacted with the endogenous β3 subunit of the vitronectin receptor expressed in Cos-7 cells as shown by the faint band detected in non transfectant cells (lane b). These results showed that the C38Y mutation should impair the complex formation or at least its normal processing as no αIIb of normal mobility could be detected.

Role of the Lys253 of the βI domain of β3 in the interaction with the αIIb β-propeller

To understand precisely the impact of the punctual mutation of Lysine 253 into Methionine, we have analyzed finely the interface between αIIb and β3 subunits. For this purpose, the protein structures obtained by Springer's group were used (PDB code 2VDL {2022}). The αIIb subunit comprises the first 452 residues and β3 from aa 109 to 352. The interface between the protein chains has a correct resolution, *i.e.* the protein resolution equals 2.75 Å and the residues implicated at the interface have all good normalized B-factor values. From a simple visualization, the side chain of the β3 Lys253 protrudes from the βA domain toward the αIIb beta-propeller surface. This residue is so in contact with different residues from the αIIb-subunit (See fig. 3A).

We used FastContact web server (http://structure.pitt.edu/servers/fastcontact/) to estimate the direct electrostatic and desolvation interaction free energy between two proteins in units of kcal/mol {2023;2024}. The computational estimation of the binding free energy is based on a statistically determined desolvation contact potential and Coulomb electrostatics with a distance-dependent dielectric constant {2023}. This free energy estimates reasonably well experimental binding affinities from complex crystal structures.

Table 4 summarizes the different results. Interestingly, the Lysine 253 has a key role in terms of binding free energy with the most negative contribution (-5.5 kcal/mol) and also in terms of electrostatics (-9.7 kcal/mol). Inversely, desolvation free energy is high (+4.1 kcal/mol). The desolvation of charged and polar amino acid is unfavorable from an energy point of view. This penalty of desolvation is here so greatly partially compensated by Coulomb interactions and by the hydrogen bonds which are formed in the complex.

Analysis of important interactions done by Lysine 253 underlines its weight in the interaction as it has the 1st (-6.7 kcal/mol with Aspartate 232 of αIIb), the 6th (-2.0 kcal/mol with Phenylalanine 231) and the 13th (-0.8 kcal/mol with Proline 238) most negative interactions of the interface. One interaction with Tryptophan 262 is slightly not favorable.

Concerning the free energy, same observations are done, with two strong interactions with Aspartate 232 (-5.5 kcal/mol) and Phenylalanine 231 (-1.2 kcal/mol). One unfavorable interaction is observed again with Tryptophan 262. These results highlight the significance of this residue that is the most important one in terms of electrostatic and free energy computation.

A structural model of Methionine 253 mutant was done and checked using ProCheck software to analyze the quality of the modification {2026}. The position of the side-chain corresponds to a preferential one as observed with SCWRL {2025}. Regarding the whole αIIb/β3 interface, the substitution provokes a striking loss of electrostatic energy (+9.1 kcal/mol) but a gain in desolvatation free energy (-5.72 kcal/mol) that cannot counter-balance the decrease of electrostatic energy. As shown in table 4, the diminution of the length of the side-chains and the change from a charged polar amino acid to a hydrophobic amino acid has a deep impact. The residue 253 has no more (negative) interaction with neither Aspartate 232, Phenylalanine 231 and Proline 238, only a single interaction with Tryptophan 262 is conserved (See fig. 3B).

From a visual point of view, the decrease of electrostatic energy between Lysine 253 (See fig. 3C) and Methionine 253 (See fig. 3D) is striking. Overall, the most important electrostatic energy implicated in the interaction becomes negligible. All these contacts are lost in presence of the Methionine excepted for the Tryptophan 262 that only preserves an electrostatic link. So these results indicate that it is rather the Lys 253 lost than the presence of the Methionine that is responsible for the complex expression defect.

DISCUSSION

The aim of the study was to identify mutations responsible for GT platelet phenotype. SDS-PAGE, western-blot and flow cytometry analyses done on patients' platelets have

confirmed GT clinical diagnosis (See table I). These patients were of various origins, Caucasian, North-African and Asian. 70 % belong to the type I GT subtype as their platelets express less than 5 % of αIIbβ3 and 25 % of fibrinogen (Fg) normal contents. Other GT patients are classified as GT type II referring to a low but significative αIIbβ3 content (< 25 %) and a relatively high level of intra-platelet Fg (≥ 50 %). The propositus 4 was shown to be heterozygous for type I GT as his platelets expressed 50 % of the normal αIIbβ3 amount and aggregated in *in vitro* testing (data not shown). The propositus 15 was fortuitously found as GT type I carrier during neonatal alloimmune thrombocytopenia diagnosis following in utero fetal death. Her platelets were phenotyped HPA-3a negative but genetically HPA-3a/b as determined by PCR-Sequence Specific Primer testing (data not shown). Thirty mutations were identified in both αIIb and β3 genes. Most of these mutations (47 %) corresponds to missense mutations but nonsense, insertion, deletion, and point mutations affecting splice sites were also found.

Several mutations which have been previously reported in the literature were identified in αIIb : c.1912_1913insT {D'Andrea, 2002 1555 /id}, c.1214T>C {D'Andrea, 2002 1555 /id}, c.1413C>G {Scott, 1998 1242 /id}, c.1787T>C {Ruan, 1998 1236 /id}, c.2113T>C {D'Andrea, 2002 1555 /id;Gonzalez-Manchon, 1999 1337 /id}, c.3060+2T>C {French, 1997 1347 /id}, c.2333A>C {Tadokoro, 1998 1296 /id}, c.2944G>A and c.2965G>A {Nurden, 2004 1631 /id}, and in β3 : c.100C>T {Negrier, 1998 1766 /id}, c.665T>C {Nurden, 2002 1733 /id}, and the double cis-acting mutations c.1143C>A and c.1260 G>A {Jin, 1996 1293 /id;1899}. Most of these mutations have not been tested in-vitro for their involvement in GT. It can be noted that their presence in patients studied herein and in 2 or 3 additionally unrelated patients would confirm their role in GT phenotype.

For the αIIb gene, 3 unpublished missense mutations were identified. Two affect the calf-2 domain of αIIb. The c.2800G>T mutation in exon 27 is responsible for the V903F substitution (Patient 6 and propositus 15). The mutation c.2870C>T in exon 28 leads to the S926L substitution (Patient 16). In both cases these mutations prevent the expression of the αIIb-β3 complex expression at the surface of Cos-7 cells. These missense mutations affect the extra-cellular N-terminal part of the αIIb β-subunit that composes the calf-2 domain. They should impair the correct folding of the Calf-2 domain as the aa Val903 and Ser926 are located in its core (See fig. 4). To estimate the importance of these two residues, an alignment of the human αIIb primary sequence with several corresponding sequences of integrins from marsupial, fish, amphibian, prochordates and insect has been done. Figure 5A shows the local alignment covering the Val903 and the Ser926 positions. These sequences share at least 45 % of identity with the αIIb (Psi-blast data from the NCBI web site) and 17 % of these residues are conserved through all the seven organisms tested. It is noteworthy that Val903 and Ser926 belong to these 17 % aa indicating that their conservation respond to a strong structural evolutionary constraint. Furthermore, their poor conservation in other human integrin α-subunit (data not shown) reinforce their α-IIb specificity.

The third so far newly described missense mutation c.1878G>C (Patient 10) affects exon 18 of αIIb gene. This homozygous exonic mutation that is contiguous with the donor splice site of intron 18 is responsible for a Q595H substitution in αIIb. No other mutation has been identified in either coding or promoter sequences of both αIIb and β3 genes. However this Q595H mutation identified in a type I GT patient does not prevent the expression of the mutant complex at the surface of transfected Cos-7 cells. It was hypothesised that the c.1878G>C mutation introduced an mRNA defect. Total RNA from patient's platelet was isolated and reverse transcribed. While full length cDNA coding for β3 was normally amplified, no PCR product was obtained for αIIb (data not shown). Splice site prediction by

NNSPLICE 0.9 cannot identify the normal donor splice site of intron 18 in the mutant. Genscan did not predict splice anomalies, but scores were lowered for both exons 18 (0.987 to 0.791) and 19 (0.995 to 0,849) implying a probability of correct splicing of 75 % instead of 99 % for the normal sequence. Jayo and coworkers {Jayo, 2006 1897 /id} reported that the 2829C>T mutation (exon 27), predicted to induce a Leu912Pro substitution, partially leads to exon 28 skipping. The authors pointed out that rather than the disruption of an ESE site, the aberrant mRNA processing would result from the strengthening of the SR protein SC35 binding score by 0.65 units (ESEFinder analysis). Interestingly ESEFinder shows the mutation 1878G>C to increase the score of an SF2/ASF binding site from 2.67 to 3.28 and to create a new one with a score of 2.50 (threshold 1.95). Finally an SRp55 binding site that encompasses the normal the normal splice sites is also created, this site presents a high score (4.33 - threshold 2.67). It can therefore be hypothesized that the 1878G>C mutation alters the normal splice factor pattern necessary to accurately splice intron 18. Splicing anomaly can lead to mRNA decay and explain the lack of detection of the mRNA coding for αIIb in patient 10.

The c.1442-13_1442-1del mutation affects the acceptor site of the intron 14 and the 11 upstream nucleotides. Its role in GT type I phenotype would be evidenced by its presence in 3 unrelated propositi, 3, 5, both type I GT, and 4, an heterozygous carrier whose platelets express 50 % of the normal amount of αIIbβ3. No family relationships was known but unknown common ancestry between them cannot be excluded as all these propositus are european caucasians and live in the north-east of France.

Genscan analysis of a genomic DNA sequence covering exons 14 to 18, predicted the retention of the intron 14 in the mutant mRNA. Unfortunately no mutant RNA from these heterozygous propositi could be isolated to verify this prediction.

The new c.917_918insA mutation (Patient 2) does not affect coding of Val275 but induces a frame shift creating a stop 22 codons downstream that is predicted to supress most of αIIb. The c.2748_2757del mutation (Patient 14) leads to a frame shift that impairs the primary sequence of the αIIb β-subunit 15 amino acids downstream its NH_2-terminal end. No stop codon could be identified in the following 552 nucleotides sequence. In both cases, the loss of a large part of αIIb can explain the GT phenotype.

The newly identified nonsense mutation C490X may provoke a large truncation of αIIb (patient 7). Nonetheless several reviews {Cartegni, 2002 1911 /id;Pagani, 2004 1912 /id} point out that nonsense mutations may result in either nonsense-mediated RNA decay (NMD) or nonsense-associated altered splicing (NAS) which could also fully explain a GT type I phenotype.

The new homozygous point mutations, αIIb c.1879-2A>G and β3 c.166-2A>G, detected in patients 9 and 19 respectively, affect splice sites themselves. Genscan analysis predicts the former mutation to lead to skipping of exon 19 and the latter to create a new acceptor splice site 37 bp dowstream in exon 3, responsible for an in frame deletion of 12 aa. As no mRNAs from these patients were available it was not possible to check for splicing defects. but the predicted changes in amin-oacid sequence or degradation of abnormally spliced mRNAs would lead to defective expression of glycoproteins. In these cases no other mutations in either αIIb and β3 genes were detected.

In the β3 gene, the homozygous 4 bp deletion c.1125+3_1125+6del (patient 25) was the single intronic mutation identified that does not directly affect a splice site. Genscan analysis predicts the use of a cryptic donor splice site located 70 bp dowstream the normal one. If this transcript is not degradated, this would lead to an in frame introduction of 23 aa between β3

β-I and hybrid domains. ESEFinder shows no modifications but NNSPLICE 0.9 suggests the contiguous donor splice site would be ignored in the mutant.

The mutation c.191G>A (patient 21) responsible for a C38Y substitution is located in the PSI domain of the β3. Transient co-transfection of the β3 mutated cDNA and with normal αIIb cDNA showed the mutation to reproduce a GT type I phenotype as no complex was detected on the cell surface by any of the anti-αIIb-β3 moab tested. Computational analysis (Genscan, ESEFinder and NNSPLICE 0.9) indicated that the c.191G>A mutation would not induce splicing modification of the pre-mRNA. Western-blot analyses showed that αIIb and mutated β3 were synthetized in transfected COS cells using moabs SZ22 and XIIF9 but retained inside the cells. The mutated Y38 β3 presents a lower relative mobility than the wild type form that could result from structural modifications induced by the C16 – C38 disulfide bond disruption. A similar observation has been reported by Valentin and co-workers {Valentin, 1995 1456 /id}, who have shown that alanine substitution of C38 lowered the relative mobility of β3 expressed in COS cells. The structural modification of the PSI domain induced by the C38Y mutation was evidenced by the lack of reactivity of moabs AP3 and SZ21 whose epitopes are respectively located in aa streches 49-98 {Peterson, 2003 1913 /id} and 28-35 {Honda, 1995 1457 /id}.

Three of the new missense mutations identified, Met118Arg, Gly221Asp and Lys253Met are located in the β-I domain of β3 and are responsible for Type I GT. The Met118 and the Gly221 are highly conserved in most integrin β subunits (data not Shown) and through invertebrates to vertebrates (See fig. 5B). Most of the β-I domain mutations previously described, are responsible for Variant {1272;1418;1412;2032;1555} or type II GT {1906;1518;1288;1416;1522}. For comparison, the figure 6 locates the mutated aa in the primary sequence (Panel A) and in the the β-I domain structure (Panel B). Whatever the variant or type II GT phenotype, the mutated aa are expressed at or partially at the surface of

the β-I domain and some of them (See fig 6B, underlined aa) present significant electrostatic or / and free energies interactions with the β-propeller (Data not shown). Variant mutations concern the MIDAS or SyMBS sites {2020} directly affecting aa involved in metal coordination (Asp119Tyr, Ser123Pro) or their very nearby environment (Arg217Trp or Gln) (See fig. 6A). Both variant and GT Type II mutations support at least a 10 % expression of αIIbβ3 at the platelet surface. This contrasts with the failure to detect the β3-Arg118 and -Asp221 forms of the complex. Both the Met118Arg and the Gly221Asp mutations, located inside the β-I domain, should deeply alter its proper folding, preventing the complex expression at the platelet surface. Due to the nature of the involved aa, these mutations induce important changes of steric hindrance and charge. However, in one case, the mutation Leu117Trp which affects 100 % buried aa still permits a 10 % expression of αIIbβ3 at the platelet surface {1286}. We could hypothesize that the characteristic of these residues, both hydrophobic and aliphatic, could explain this behavior. At the opposite for the Gly221Asp mutation, changes of volume and charge of the side-chains has a too deep impact. Similarly, such a steric hindrance change could explain the type I phenotype induced by the Meth124Val mutation {1678}. as the Met124 sidechain pointed inward the β-I domain.

Unlike for the Met118 and the Gly221, the Lys253 is not conserved in other integrin β subunits and if it is present in β3 from fishes to primates it is replaced by an Arg in amphibian and absent from invertebrate integrins. However the Lys253Met substitution results in type I GT. The 3-dimensional structure of the αIIbβ3 headpiece revealed that the side chain of the Lys253 protrudes from the β-I domain toward a pocket at the surface of the αIIb β-propeller (See fig. 3a and 6). Analyses of electrostatic, desolvation and free energies revealed that the Lys253 is one of the most important aa involved in the β-I domain interaction with the β-propeller of αIIb. Furthermore, a mutant model of the αIIbβ3 headpiece shows that the Lys253 substitution by a Met does not introduce steric and energetic clashes but only

suppresses important contacts with the αIIb β-propeller. So the Lys253Met mutation revealed the Lys253 as a key aa for the association of the β-I domain with the β-propeller. The last so far reported mutation of the β-I domain that lead to type I GT was a substitution of the sequence Ile325-Pro326-Gly327 by methionine. This mutation impairs the αIIb / β3 association {1064}. However, the mutated aa locates between the α6 helix and the β7 sheet and do not directly face the αIIb β-propeller surface (See fig. 6B). Furthermore the Ile325-Pro326-Gly327 sequence does not seem to have significant if any, interaction with the β-propeller as indicated by free and electrostatic energy analysis (data not shown). It might indirectly impair the interaction(s) of the α5 and / or α6 helix with the β-propeller. The last four described mutations Lys137Gln {2021}, Thr140Ile (HPA-16bw) {1521}, Arg143Gln (HPA-4) {1171} and Thr195Asn (HPA-17bw) {2002} only lead to allelic avriants involved in alloimmune thrombocytopenia that are not related to GT phenotype. All these aa locate at the surface of the β-I domain with their side chains directed outside.

In conclusion, we have identified 30 mutations in a panel of 24 GT patients and 2 GT carriers. Eighteen of these mutations have not been described so far. We have confirmed by *in vitro* studies that the identified missense mutations impaired normal expression of the mutant complex (except for one case). Nonsense and splice site mutations were considered to be related to the GT phenotype. This study emphasizes the high allelic heterogeneity of both the αIIb and β3 genes involved in GT phenotype. Finally the GT variant Lys253Met of β3 unveiled the key role of the Lys 253 in the β-propeller / β-I association of the αIIbβ3 headpiece.

Aknowledgments

We thank the following colleagues for sending us blood samples from the patients we have studied here-in : B. Bastenaire, C. Caron, M. Dreyfus, F. Dutrillaux, I Elalami, Nizard, G. Le Roux, J. Peynet, S. C. Saladin-Thiron / MT Bricquet, P. Tron, J.P. Vernant. We also thank the following technician students for their help in mutation identification : M. Brément, S. Cantais, E. Divron, F. Jacquinot, A. Ledigarcher, P. Moffat, V. Noel and F. Ping.

Table 1 : Propositi informations

Patient	Sex	Origin	GP IIb (%)	GP IIIa (%)	GP Ib (%)	fg[a] (%)	GT type
1	M	China	< 5	< 5	100	15	I
2	F	Cauc Eur[b]	NT[d]	NT[d]	NT[d]	NT[d]	I
3	M	Cauc Eur[b]	NT[d]	NT[d]	NT[d]	NT[d]	I
4	F	Cauc Eur[b]	53	66	100	100	I (carrier)
5	F	Cauc Eur[b]	< 5	< 5	100	NT	I
6	M	Cauc Eur[b]	< 5	< 5	100	15	I
7	F	Cauc Eur[b]	< 5	11	100	11	I
8	NC[e]	NC	NC[e]	NC[e]	NC[e]	NC[e]	NC[e]
9	F	Kuwait	NT[d]	NT[d]	NT[d]	NT[d]	I
10	F	North Afri[c]	< 5	< 5	100	15	I
11	F	Cauc Eur[b]	< 5	20	100	3	I
12	F	Cauc Eur[b]	19	40	100	51	II
13	M	Japan	< 5	< 5	100	49	I
14	F	North Afri[c]	< 5	< 5	100	15	I
15	F	Cauc Eur[b]	NT[d]	NT[d]	NT[d]	NT[d]	I (carrier)
16	M	North Afri[c]	2	10	100	15	I
17	M	North Afri[c]	13	27	100	NT[d]	II
18	NC[e]	NC[e]	NC[e]	NC[e]	NC[e]	NC[e]	NC[e]
19	NC[e]	NC[e]	NC[e]	NC[e]	NC[e]	NC[e]	NC[e]
20	M	North Afri[c]	< 5	< 5	100	< 5	I
21	M	Cauc Eur[b]	< 5	< 5	100	24	I
22	F	Colombia	< 5	< 5	100	15	I
23	F	Cauc Eur[b]	10	14	100	83	II
24	F	North Afri[c]	< 5	10	100	13	I
25	NC[e]	NC[e]	NC[e]	NC[e]	NC[e]	NC[e]	NC[e]
26	F	North Afri[c]	12	12	100	NT	I

[a]fg : intraplatelet fibrinogen
[b]Cauc Eur : Caucasian european
[c]North Afri : North African
[d]NT : Not tested
[e]NC : Not communicated

Table 2 : αIIb mutations identified by genomic analysis[a]

Proband	Exon /intron[b]	Sequence alteration[c]	Restriction enzyme	Predicted effect (HGVS)[d]	Predicted effect (Classical)[e]
1	Ex 4	c.531T > A	Hga I	p.Cys171X	C146X
2	Ex 10	c.917_918ins A	Alw I	Gln306GlnfsX22	Q275 + FS[h]
	Ex19	c.1912_1913ins T	No enzyme	Val638ValfsX22	V607 + FS[h,i]
3	Ex 13	c.1214T > C	Sfc I	p.Ile405Thr	I374T[i]
	IVS14	c.1442-13_1442-1del	Hph I	Splice[f]	Splice[f]
4	IVS14	c.1442-13_1442-1del	Hph I	Splice[f]	Splice[f]
5	IVS14	c.1442-13_1442-1del NI[g]	Hph I	Splice[f]	Splice[f]
6	Ex 14	c.1413C > G	Dde I	p.Tyr471X	Y440X[j]
	Ex 27	c.2800G > T	Mae III / Tsp45 I	p.Val934Phe	V903F
7	Ex 16	c.1563T > A NI[g]	No enzyme	p.Cys521X	C490X
8	Ex 17	c.1672C>T	Mse I	p.Gln558X	Q527X
9	IVS18	c.1879-2A > G	Xba I	Splice[f]	Splice[f]
10	Ex 18	c.1878G > C	Hpy CH IV	Gln626His / Splice[f]	Q595H / Splice[f]
11	Ex 18	c.1787T > C	No enzyme	p.Ile596Thr	I565T[k]
12	Ex 21	c.2113T > C	Fok I	p.Cys705Arg	C674R[i,l]
	IVS29	c.3060+2T>C	Hph I	Val982_Lys1020del	V951_K989del[m]
13	Ex 23	c.2333A > C	Bsr I / TspR I	p.Gln778Pro	Q747P[n]
14	Ex 27	c.2748_2757del	Rsa I	Thr917Serfs	T886S + FS[h]
15	Ex 27	c.2800G > T	Mae III / Tsp45 I	p.Val934Phe	V903F
16	Ex 28	c.2870C > T	Hpy CH4 V	p.Ser957Leu	S926L
17	Ex 28	c.2929C > T NI[g]	Ava I	p.Arg977X	R946X
18	Ex 29	c.2944G >A	Bst NI	p.Val982Met	V951M[o]
	Ex 29	c.2965G > A NI[g]	Nci I	p.Ala989Thr	A958T[o]

[a]cdNA ITG2B GenBank accession number NM_000419.3
[b]Ex : Exon ; IVS : intronique sequence
[c]Nomenclature according to HGVS : +1 corresponds to the A of ATG translation initiation codon
[d]Nomenclature according to HGVS : +1 corresponds to the initiating Met (signal peptide includes)
[e]Classical nomenclature : +1 corresponds to the first amino acid of the mature αIIb
[f]Splice defect based upon modelization with GENSCAN / NNSPLICE and ESEFinder
[g]NI : 2nd mutation not Identified
[h]FS : Frame shift
References : [i]{1555}; [j]{1242}; [k]{1236} ; [l]{1337} ; [m]{1347} ; [n]{1296} ; [o]{1631}

Table 3 : β3 mutations identified by genomic analysis[a]

Proband	Exon /intron[b]	Sequence alteration[c]	Restriction Enzyme	Predicted effect (HGVS)[d]	Predicted effect (Classical)[e]
19	IVS2	c.166-2 A>G	Apa I	Splice[f]	Splice[f]
20	Ex 2	c.100 C > T	Hpy CH4 IV	Arg34X	R8X[h]
21	Ex 3	c.191 G > A NI[g]	Tsp 45I	Cys64Tyr	C38Y
22	Ex 4	c.431 T > G	Bsm F1	Met144Arg	M118R
23	Ex 5	c.665 T > C	Acy I	Leu222Pro	L196P[i]
24	Ex 5	c.740 G > A	Fok I	Gly247Asp	G221D
	Ex 6	c.836 A > T	Fat I	Lys279Met	K253M
25	IVS8	c.1125+3_1125+6del NI[g]	No enzyme	Splice[f]	Splice[f]
26	Ex 9	c.1143 C>A	Taq I	K376_T420del	K350_T394del[j]
	Ex 9	c.1260 G>A	Hph I		

[a]cdNA ITGB3 GenBank accession number NM_000212.2
[b]Ex : Exon ; IVS : intronique sequence
[c]Nomenclature according to HGVS : +1 corresponds to the A of ATG translation initiation codon
[d]Nomenclature according to HGVS : +1 corresponds to the initiating Met (signal peptide includes)
[e]Classical nomenclature : +1 corresponds to the first amino acid of the mature β3
[f]Splice defect based upon modelization with GENSCAN, NNSPLICE and ESEFinder
[g]NI : 2nd mutation not Identified
References : [h]{1766} ; [i]{1733} ; [j]{1293}

Table 4 : Energetic effects of the Lys 253 Met substitution in the αIIb/ β3 interaction

		Lys 253			Met 253		
Energy of :		**Rank**	**Value (kcal/mol)**	**αIIb contact**	**rank**	**Value (kcal/mol)**	**αIIb contact**
αIIb-β3 Interface	**Electrostatic (4r) Energy**	/	-25.14	/	/	-16.08	/
	Desolvation Free Energy	/	-1.09	/	/	-6.81	/
	Van der Waals (CHARMm19)	/	-4894.63	/	/	-4903.95	/
Residue	**Binding free energy**	1st negative	-5.541	/	12th negative	-1.309	/
	Desolvation free energy	1st positive	4.124	/	6th negative	-1.347	/
	Electrostatics energy	1st negative	-9.666	/	/	*low*	/
Contact	**Electrostatic**	1st negative	-6.715	232 ASP	/	/	/
		6 th negative	-2.076	231 PHE	/	/	/
		13th negative	-0.788	228 PRO	/	/	/
		10th positive	0.670	262 TRP	6th negative	-0.935	262 TRP
	Free energy	1st negative	-5.517	232 ASP	/	/	/
		8th negative	-1.166	231 PHE	/	/	/
		2th positive	2.057	262 TRP	/	/	/

Figure :

Figure 1 : Flow cytometric analysis of the expression of the mutant forms of αIIb-β3. Transiantly transfected COS-7 cells expressing the wild type (WT) or the following mutant of αIIb-β3, S926L, Q595H, V903F (αIIb) and C38Y, M118R, G221D, K253 (β3) were tested in flow cytometry by using the moabs SZ22 (Hacthed bar), SZ21 (Dot bar) and P2 (White bar) or irrelevante mouse IgG (Black bar). As a control untransfected cells (NT) were also tested. Following Moab incubation, bound IgGs were detected by using a polyclonal goat anti-mouse IgG conjugated to FITC. Washed cells were analysed on an Epic-XML flow cytometer. Except for the αIIb Q595H one, all mutants showed a markedly decreased expression of the complex when compared to the wild type.

Figure 2 : Western blot analysis of the Y38 β3 form of the αIIb-β3 complex expressed in COS-7 cells. SDS lysates from normal platelets (lane a), non-transefected COS-7 cells (lane b), or COS-7 cells expressing the wild-type (lane c) or the Y38 β3 (lane d) forms of the complexe were subjected to SDS-polyacrylamide gel electrophoresis under non reduced conditions and transferred to nitrocellulose membrane. Following incubation with Moabs SZ22, XIIF9, SZ21 and AP3, membrane bound IgGs were revealed by using anti-mouse IgG conjugated to peroxidase and the enhanced chemiluminescence detection technique.

Figure 3 : Location and modelization of the electrostatic effect of the Lys 253 Met substitution. (A) and (B) Ribon diagram of the αIIb β-propeller (in blue) and β3 βI (in red) complexed domains. For the βI domain, The residue 253 is shown in green with (A) Lys 253 and (B) Met 253, while for β-propeller partners the Pro 228 is shown in yellow, the Phe 231 in grey, the Trp 262 in pink and the Asp 232 in orange. (C) and (D) Electrostatics

visualization of the punctual mutation Lys 253 Met with (C) wild β3 subunit with Lys 253 and (D) wild β3 subunit with Met 253. The visualizations are done using PyMol software (http://www.pymol.org).

Figure 4 : Localization of the V903 and S926 on a ribbon diagram of αIIb. This αIIb cartoon shows the internal location of the V903 and S926 side chains (orange, ball and stick representation) in the calf-2 composed by the N-terminal part of the β-subunit of αIIb (blue) and the C-terminal part of the α-subunit (yellow and red respectively for β-sheet and α-helix). This ribbon diagram was obtained from the resolved structure of αIIb (PDB code 3FCS) using the Swiss-PdbViewer software (Version 4.0.1).

Figure 5 : Sequence conservation of the amino-acids mutated. Shown are partial protein sequence alignments of αIIb (panel A) and β3 (panel B) regions from human (gi 190068/αIIb and 47078292/β3), marsupial (gi 126308484 and 126308601), amphibian (gi 209969730 and 148234631), fish (gi 1008138 and 130504431), Amphioxus (gi 210105285 and 219437062), insect (gi 195457234 and 304789) and tunicate (gi 12583701 and 198420437). Amino acids of interest are boxed and high, low and neutral consensus residues are respectively red, blue and black. Except for the Lys 253 of the β3 subunit, all concerned (boxed) aminoacids were highly conserved. Sequences were identified by using Psi-blast (with the non-redondant protein sequence data base) from the NCBI web site (www.ncbi.nlm.nih.gov) and multiple alignments were generated with Multalin (http://bioinfo.genotoul.fr/multalin/multalin.html).

Figure 6 : Localization of the allelic variants of the β-I domain of β3. Residues identified in this study and from the literature as involved in GT or neonatal alloimmune thrombocytopenia and that locate in the β-I domain of β3 are reported on its primary sequence

(panel A) and a ribbon diagrams showing the β-I domain and a partial view of the β-propeller of αIIb (Panel B). Allelic variants of residues highlighted in magenta, blue, green are respectively responsible for variant, II and I GT phenotypes or yellow for those concerning alloimmunisation. The GT type induced by the allelic variant of the H192 (grey) is not reported {1899}. Amino-acids identified by the energetical study as in contact with the αIIb β-propeller are underlined. The primary sequence (Panel A) identifies the secondary structures and amino-acids responsible for MIDAS (★), ADMIDAS (●) and SyMBS (♦) sites. As known, variant GT mutations GT specifically affect metal ion binding sites but other mutants concern residues evenly distributed along the primary sequence. Boxed residues have been identified in this study. The ribbon diagram (Panel B) was obtained from the resolved structure of αIIb (PDB file 2VDL) using the Swiss-PdbViewer software (Version 4.0.1). α-helix (red) and β-sheet (yellow) are shown. All residues whose mutants are involved in type II GT lay on the β-I surface except for the L117, some of them (underlined amino-acids) directly contacting the β-propeller. The Met 118 and Gly 221 locate inside the β-I domain and the Lys 253 points out to the β-propeller surface however their identified allelic variants completely prevent the αIIbβ3 complex expression at the platelet surface.

Fig 2

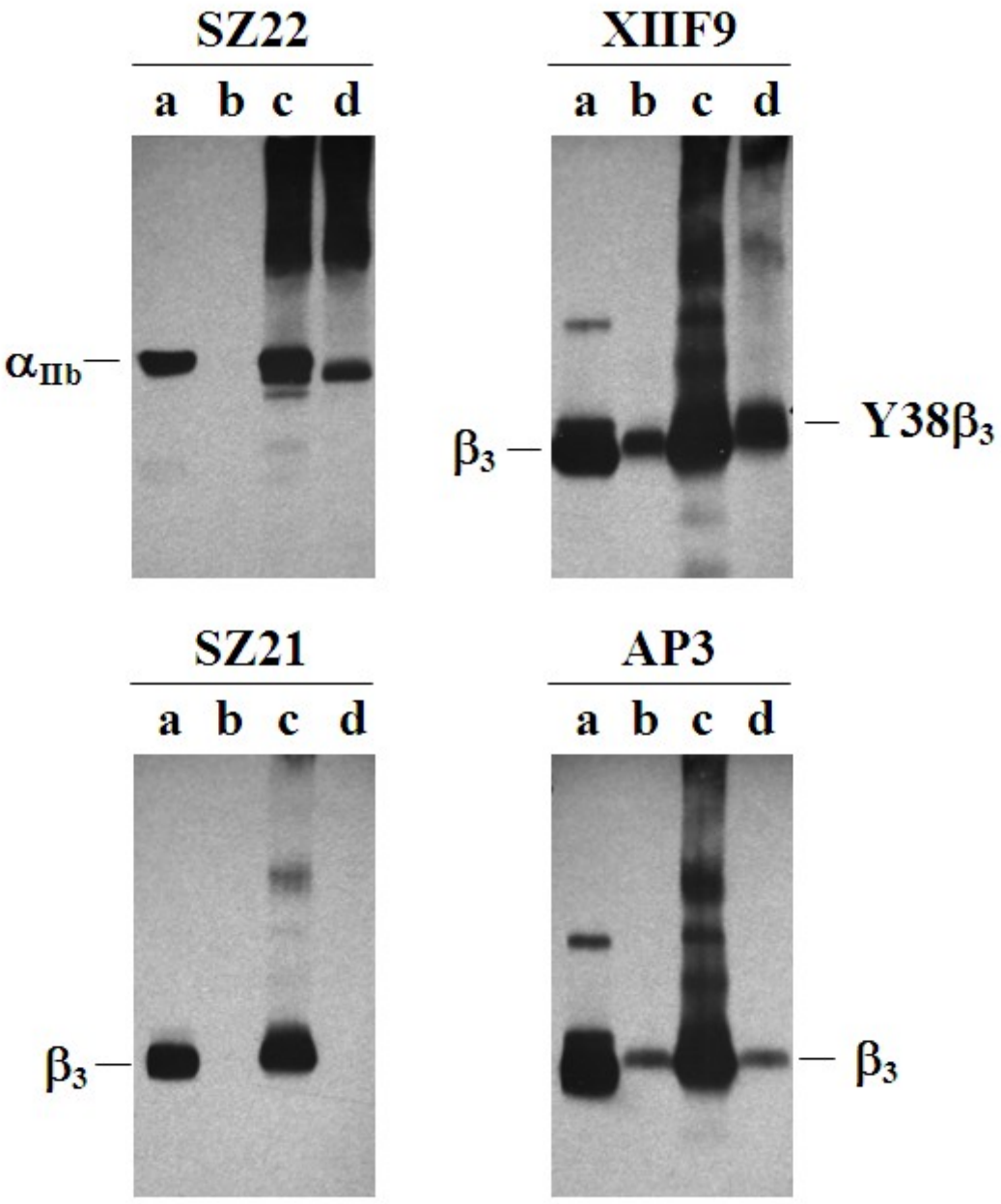
SZ22
a b c d
α_{IIb}
XIIF9
a b c d
β_3
Y38β_3
SZ21
a b c d
β_3
AP3
a b c d
β_3

Fig 3

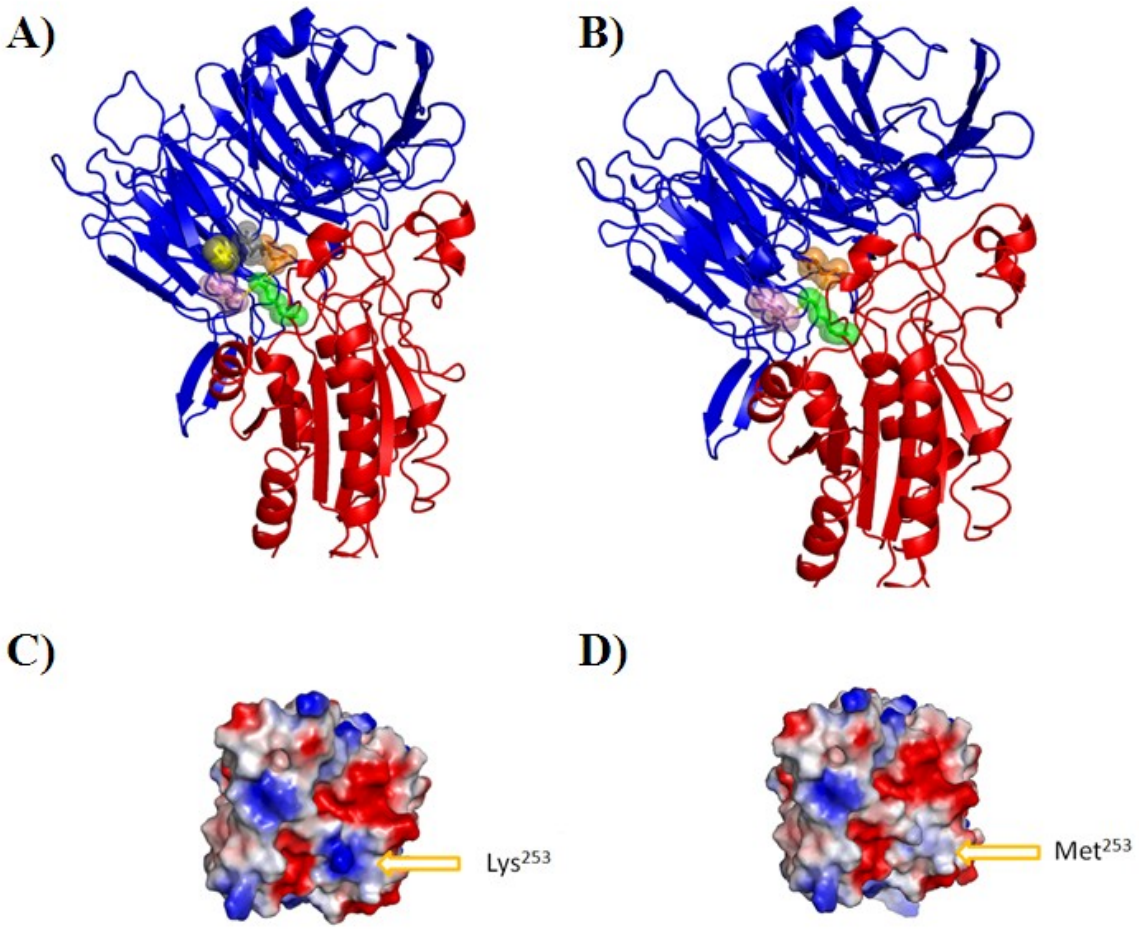

Fig 4

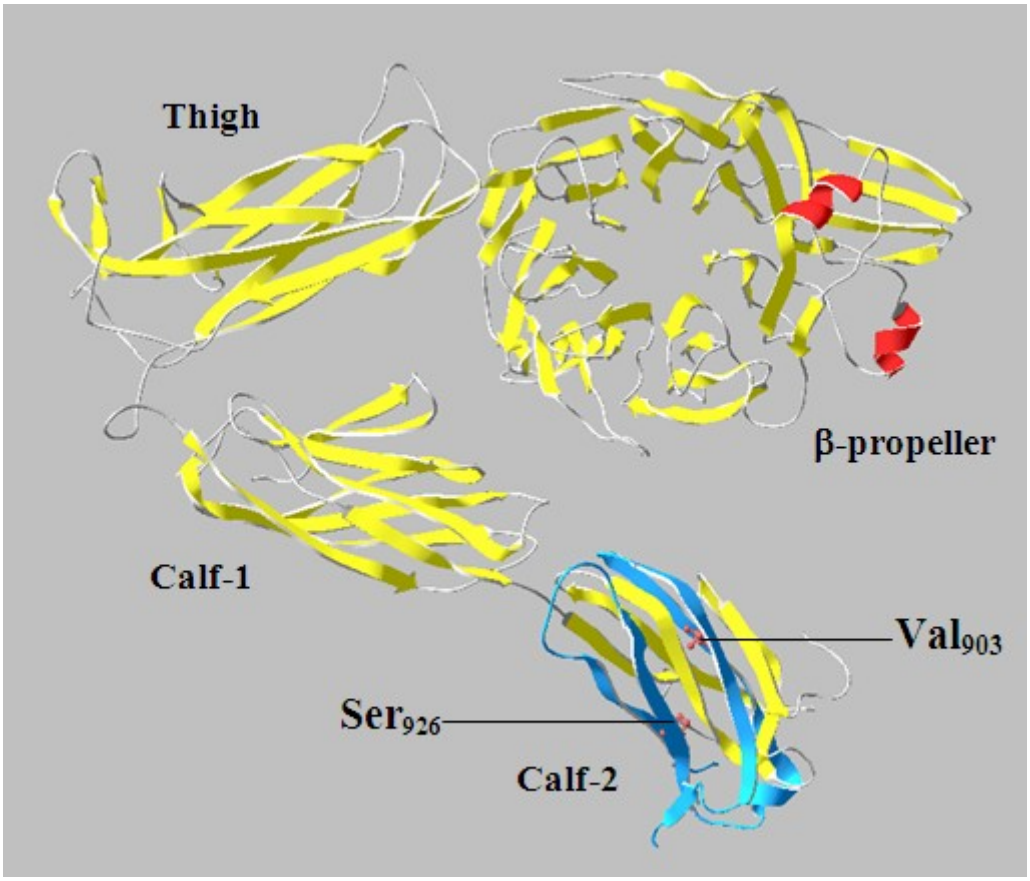

Fig 5

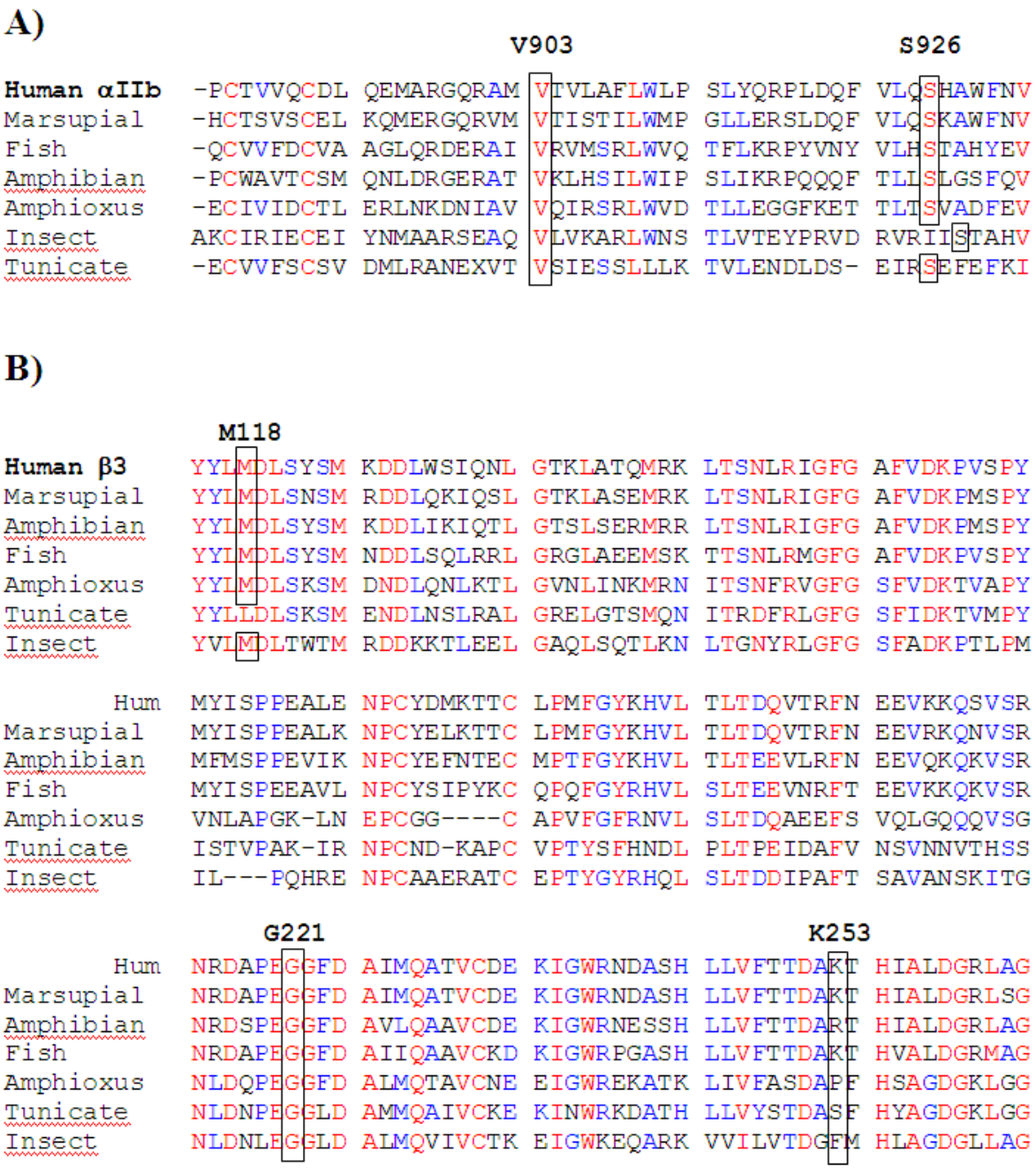
A)
V903
S926
Human αIIb -PCTVVQCDL QEMARGQRAM VTVLAFLWLP SLYQRPLDQF VLQSHAWFNV
Marsupial -HCTSVSCEL KQMERGQRVM VTISTILWMP GLLERSLDQF VLQSKAWFNV
Fish -QCVVFDCVA AGLQRDERAI VRVMSRLWVQ TFLKRPYVNY VLHSTAHYEV
Amphibian -PCWAVTCSM QNLDRGERAT VKLHSILWIP SLIKRPQQQF TLLSLGSFQV
Amphioxus -ECIVIDCTL ERLNKDNIAV VQIRSRLWVD TLLEGGFKET TLTSVADFEV
Insect AKCIRIECEI YNMAARSEAQ VLVKARLWNS TLVTEYPRVD RVRIISTAHV
Tunicate -ECVVFSCSV DMLRANEXVT VSIESSLLLK TVLENDLDS- EIRSEFEFKI
B)
M118
Human β3 YYLMDLSYSM KDDLWSIQNL GTKLATQMRK LTSNLRIGFG AFVDKPVSPY
Marsupial YYLMDLSNSM RDDLQKIQSL GTKLASEMRK LTSNLRIGFG AFVDKPMSPY
Amphibian YYLMDLSYSM KDDLIKIQTL GTSLSERMRR LTSNLRIGFG AFVDKPMSPY
Fish YYLMDLSYSM NDDLSQLRRL GRGLAEEMSK TTSNLRMGFG AFVDKPVSPY
Amphioxus YYLMDLSKSM DNDLQNLKTL GVNLINKMRN ITSNFRVGFG SFVDKTVAPY
Tunicate YYLLDLSKSM ENDLNSLRAL GRELGTSMQN ITRDFRLGFG SFIDKTVMPY
Insect YVLMDLTWTM RDDKKTLEEL GAQLSQTLKN LTGNYRLGFG SFADKPTLPM
Hum MYISPPEALE NPCYDMKTTC LPMFGYKHVL TLTDQVTRFN EEVKKQSVSR
Marsupial MYISPPEALK NPCYELKTTC LPMFGYKHVL TLTDQVTRFN EEVRKQNVSR
Amphibian MFMSPPEVIK NPCYEFNTEC MPTFGYKHVL TLTEEVLRFN EEVQKQKVSR
Fish MYISPEEAVL NPCYSIPYKC QPQFGYRHVL SLTEEVNRFT EEVKKQKVSR
Amphioxus VNLAPGK-LN EPCGG----C APVFGFRNVL SLTDQAEEFS VQLGQQQVSG
Tunicate ISTVPAK-IR NPCND-KAPC VPTYSFHNDL PLTPEIDAFV NSVNNVTHSS
Insect IL---PQHRE NPCAAERATC EPTYGYRHQL SLTDDIPAFT SAVANSKITG
G221
K253
Hum NRDAPEGGFD AIMQATVCDE KIGWRNDASH LLVFTTDAKT HIALDGRLAG
Marsupial NRDAPEGGFD AIMQATVCDE KIGWRNDASH LLVFTTDAKT HIALDGRLSG
Amphibian NRDSPEGGFD AVLQAAVCDE KIGWRNESSH LLVFTTDART HIALDGRLAG
Fish NRDAPEGGFD AIIQAAVCKD KIGWRPGASH LLVFTTDAKT HVALDGRMAG
Amphioxus NLDQPEGGFD ALMQTAVCNE EIGWREKATK LIVFASDAPF HSAGDGKLGG
Tunicate NLDNPEGGLD AMMQAIVCKE KINWRKDATH LLVYSTDASF HYAGDGKLGG
Insect NLDNLEGGLD ALMQVIVCTK EIGWKEQARK VVILVTDGFM HLAGDGLLAG

Fig 6

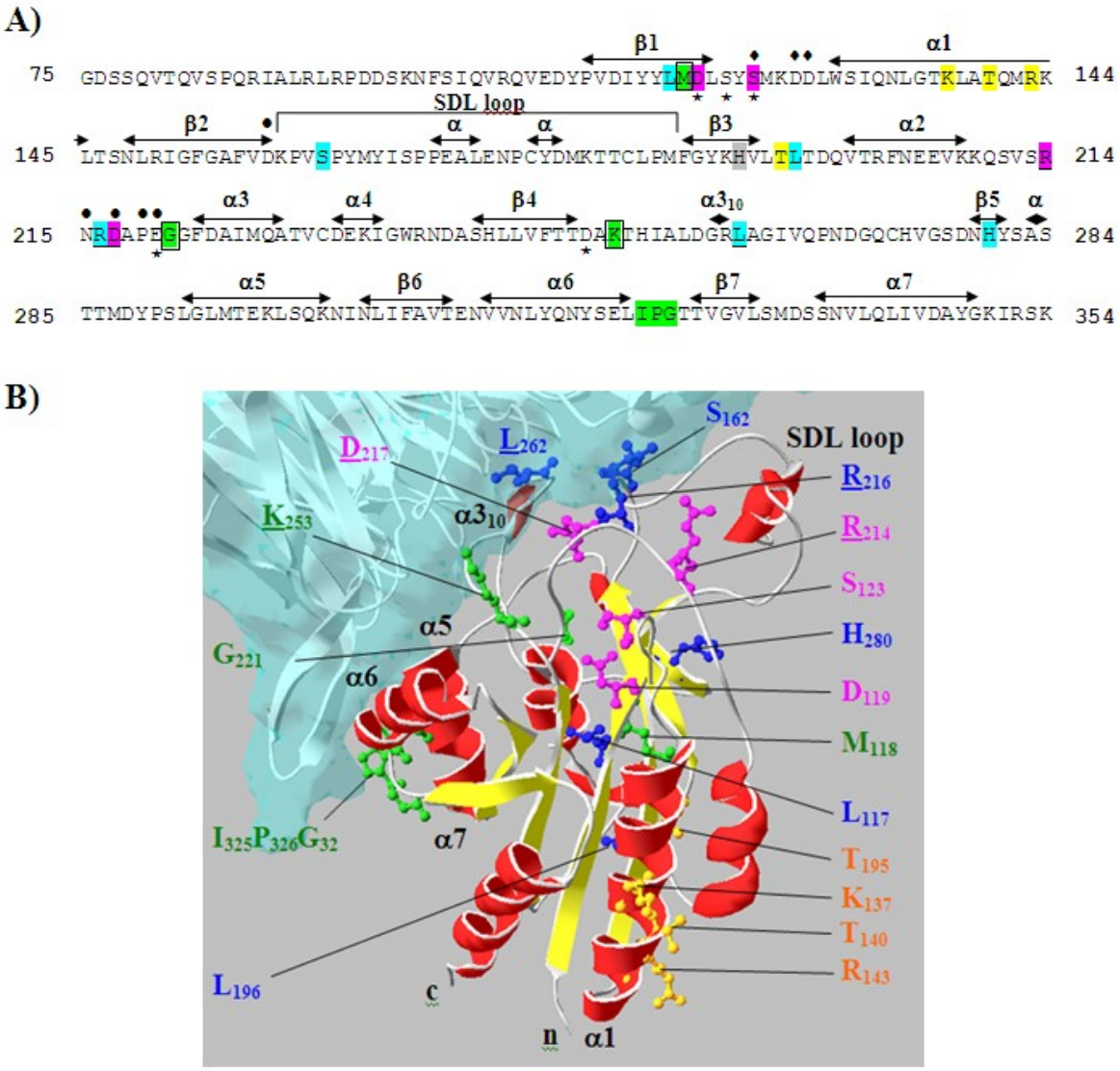
A)
β1
α1
75 GDSSQVTQVSPQRIALRLRPDDSKNFSIQVRQVEDYPVDIYYLMDLSYSMKDDLWSIQNLGTKLATQMRK 144
SDL loop
β2
α
α
β3
α2
145 LTSNLRIGFGAFVDKPVSPYMYISPPEALENPCYDMKTTCLPMFGYKHVLTLTDQVTRFNEEVKKQSVSR 214
α3
α4
β4
α3₁₀
β5
α
215 NRLAPEGGFDAIMQATVCDEKIGWRNDASHLLVFTTDAKTHIALDGRLAGIVQPNDGQCHVGSDNHYSAS 284
α5
β6
α6
β7
α7
285 TTMDYPSLGLMTEKLSQKNINLIFAVTENVVNLYQNYSELIPGTTVGVLSMDSSNVLQLIVDAYGKIRSK 354
B)
S162
SDL loop
D217
L262
R216
K253
α3₁₀
R214
S123
α5
H280
G221
α6
D119
M118
L117
I325P326G32
α7
T195
K137
T140
L196
R143
c
n
α1